Supporting Information

On-Surface Chemistry of Pb(II) Tetraphenylporphyrin on Au(111): Reversible Metalation, Thermal Degradation, and Formation of a Covalent Organic Framework

Jan Herritsch, Cong Guo, Lukas J. Heuplick, Mark Hutter, Qitang Fan, Florian Münster, Stefan R. Kachel, Malte Zugermeier, J. Michael Gottfried

Fachbereich Chemie, Philipps-Universität Marburg,
Hans-Meerwein-Straße 4, 35032 Marburg, Germany

Table of contents

S1 Background treatment of the Pb 4f XPS spectra S2

S2 Calculated valence electronic structure of Pb(TPP) S3

S3 Further Details on the Adsorbate Interactions of Pb(TPP) on Au(111) S4

S4 Additional XPS spectra of the thermal-induced on-surface reaction of a Pb(TPP) monolayer on Au(111) S5

S5 Details on the N 1s fitting procedure S6

S6 Comparison of the adsorbate structure of a Pb(TPP) monolayer after heating to 550 K and a H2(TPP) monolayer on Au(111) S6

S7 Additional XPS spectra of the on-surface metalation of H2(TPP) with Pb and the on-surface reaction after thermal treatment S7

References S9

S1 Background treatment of the Pb 4f XPS spectra

In the case of the monolayer spectra, a background correction was applied to the Pb 4f core-level spectra (Fig. S1). A spectrum of the clean Au(111) substrate was interpolated using a smoothing spline. This background was then scaled to match the experimental data in the lower binding energy region (130 eV to 132 eV) and subsequently subtracted from the corresponding monolayer spectra.

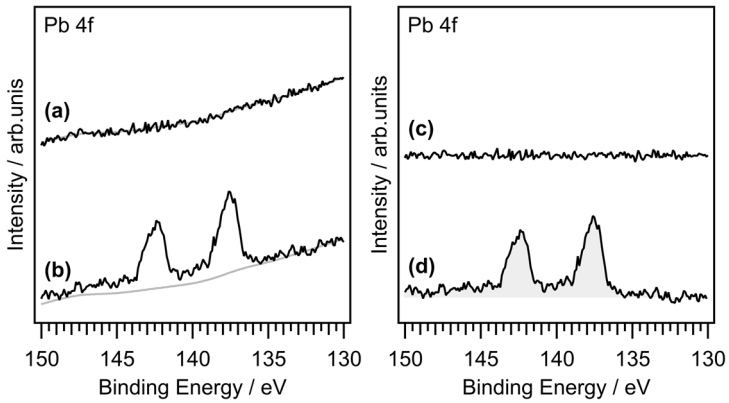

Fig. S1. (a) XPS spectrum in the Pb 4f region of the clean Au(111) substrate; (b) Pb(TPP) monolayer XPS spectrum. (c, d) Corresponding XPS spectra after the background correction. The black line in (a) and (b) represents the raw spectrum, while the gray line depicts the smoothing spline background, which has been subtracted.

S2 Calculated valence electronic structure of Pb(TPP)

DFT calculations were performed with Gaussian16, A.03[1] using the PBE[2] functional and the def2-TZVPP[3-5] basis set. The "tight" convergence criteria and an "ultrafine" integration grid were applied in this regard. The def2-TZVPP[3-5] basis set was used for the light elements (N, C, H). For Pb, def2-TZVPP was used in combination with a relativistic pseudopotential (def2-ECP)[6] to account for relativistic effects.

Gas-phase DFT calculations were used to visualize the valence electronic structure of Pb(TPP), see Fig. S4. The HOMO−2 in particular is of a paramount importance here, as it has the largest overlap with the metal substrate and will be relevant for the adsorbate interactions of the Pb-down isomer. In case of the Pb-up isomer, the HOMO−2 is responsible for the pronounced contrast at the metal center in STM images and also determines the reactivity towards an additional axial coordination at the Pb center.

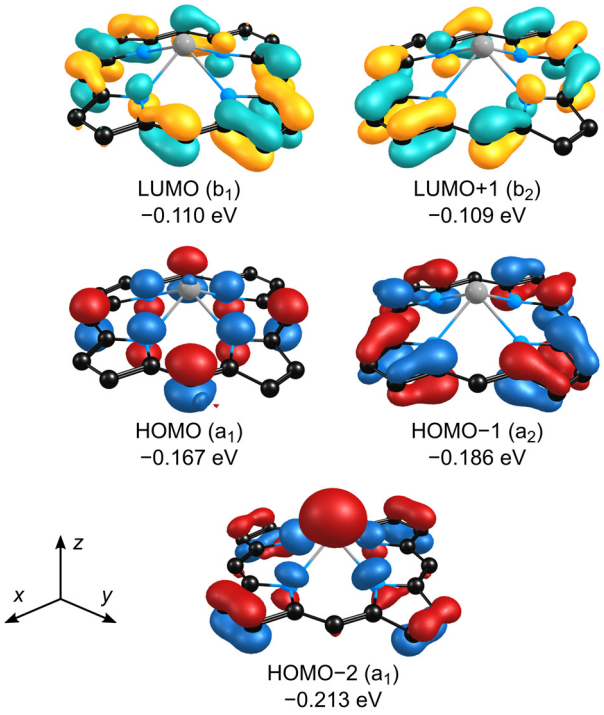

Fig. S2. Selected molecular orbitals (isovalue = 0.04) of Pb(TPP) derived from gas phase DFT calculations. Phenyl substituents and hydrogen atoms are included in the calculation but were omitted for the sake of clarity. The given energy eigenvalues refer to the vacuum level. Due to the non-planar structure with the out-of-plane bound metal center and the orientation of the phenyl rings, the molecule exhibits approximately C_{2v} symmetry, and the labels in parentheses refer to the molecular orbitals' irreducible representations of a C_{2v} symmetry within the shown coordinate system.

S3 Further Details on the Adsorbate Interactions of Pb(TPP) on Au(111)

Based on experimental and theoretical literature findings for Sn(Pc) on Ag(111)[7, 8], which has a similar structure to the Pb(TPP) with an out-of-plane bound metal center, we conclude that the Pb↓ structure exhibit a strong covalent bond towards the metal substrate, while the Pb↑ structure show a weaker, van-der-Waals dominated adsorbate interaction.

The covalent interaction between the Sn↓ configuration of Sn(Pc) and Ag(111) has previously been attributed to the donor bond of the molecule's Sn 5s-type orbital and the Ag surface.[8] DFT calculations of a Au··Pb(TPP) complex in the gas phase suggest a similar interaction in the case of Pb(TPP) on Au(111) (Fig. S3). The formerly fully occupied HOMO−2 of Pb(TPP) mixes with the Au 6s atomic orbital, forming an anti-bonding orbital that corresponds to the singly occupied a_1-type orbital (SOMO). Furthermore, the orbital is shifted upwards in energy and is only singly occupied.

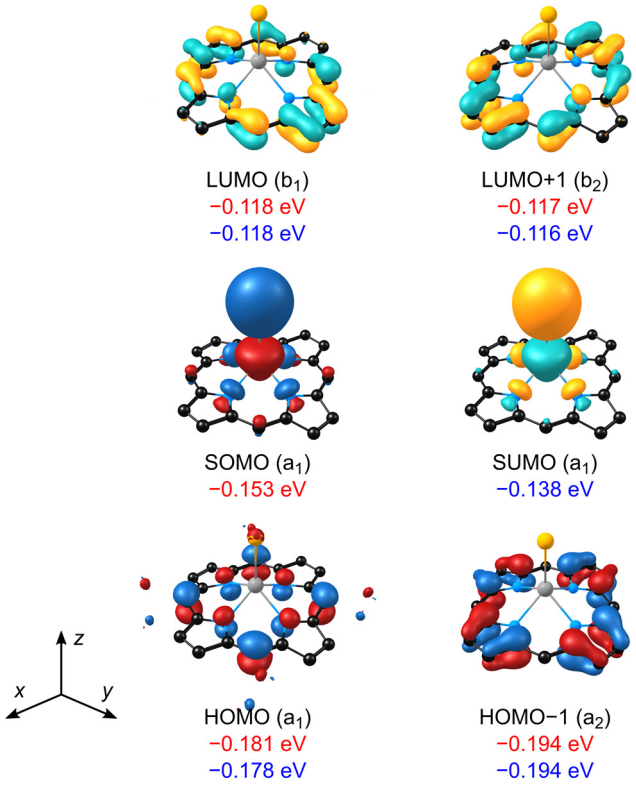

Fig. S3. Selected molecular orbitals (isovalue = 0.04) of a Au··Pb(TPP) complex derived from gas phase DFT calculations. Phenyl substituents and hydrogen atoms are included in the calculation but were omitted for the sake of clarity. The given energy eigenvalues of the alpha (beta) spin channel are denoted in red (blue) and refer to the vacuum level. The complex exhibits approximately C_{2v} symmetry, and the labels in parentheses refer to the molecular orbitals' irreducible representations of a C_{2v} symmetry within the shown coordinate system.

S4 Additional XPS spectra of the thermal-induced on-surface reaction of a Pb(TPP) monolayer on Au(111)

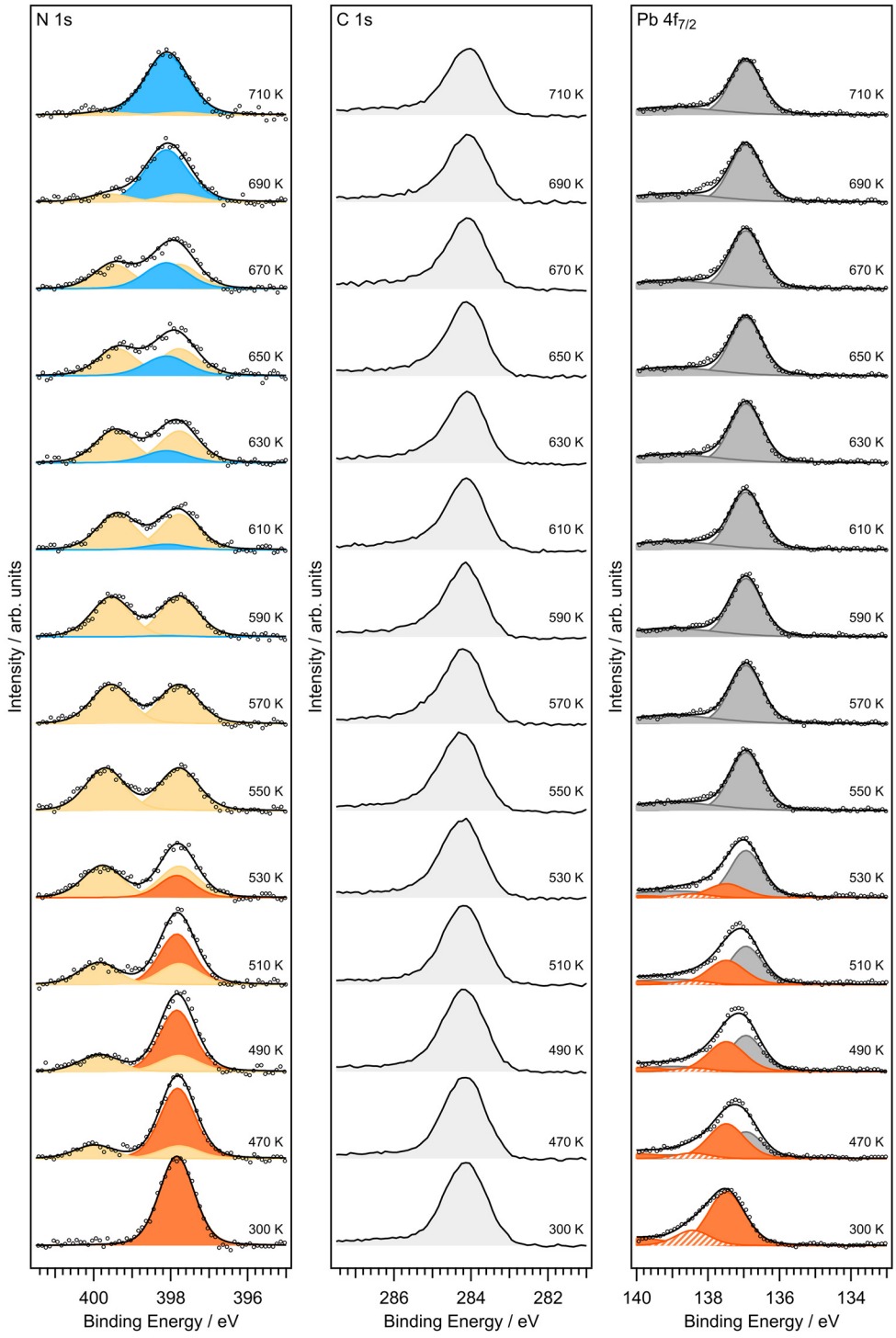

Fig. S4. Temperature-dependent XPS spectra of the directly deposited Pb(TPP) monolayer on Au(111). The N 1s region is described by a fitting procedure taking into account the intact Pb(TPP) (orange), unmetalated porphyrin species (beige) and remetalated macrocycles (blue). The C 1s signal does not show any significant changes during the reactions. The Pb 4f region is described by the Pb(TPP) (orange) and the reduced Pb(0) indicating an non-reversable reduction of the initial Pb(II) species.

S5 Details on the N 1s fitting procedure

The temperature induced transformation of the porphyrin's N_4 coordination site was derived from the N 1s region by a fit function taking into account Pb(TPP), H_2(TPP) and Au(porphyrin) species. Pb(TPP) is described by a single peak at a binding energy of 397.8 eV. The demetalation product H_2(TPP) exhibit two components; the pyrrolic species (−NH−) at 400.0 eV and the iminic species (−N=) at 397.8 eV. The 1:1 ratio of the signal intensity of the pyrrolic/iminic species was kept constant. However, the peak positions show a temperature dependency due to the thermal-induced dehydrogenation of the peripheral ligand backbone and, thus, were not kept constant at temperatures above 470 K. At temperatures above 570 K, the formation of Au(porphyrin) species were considered by a single peak at a binding energy of 398.1 eV.

S6 Comparison of the adsorbate structure of a Pb(TPP) monolayer after heating to 550 K and a H_2(TPP) monolayer on Au(111)

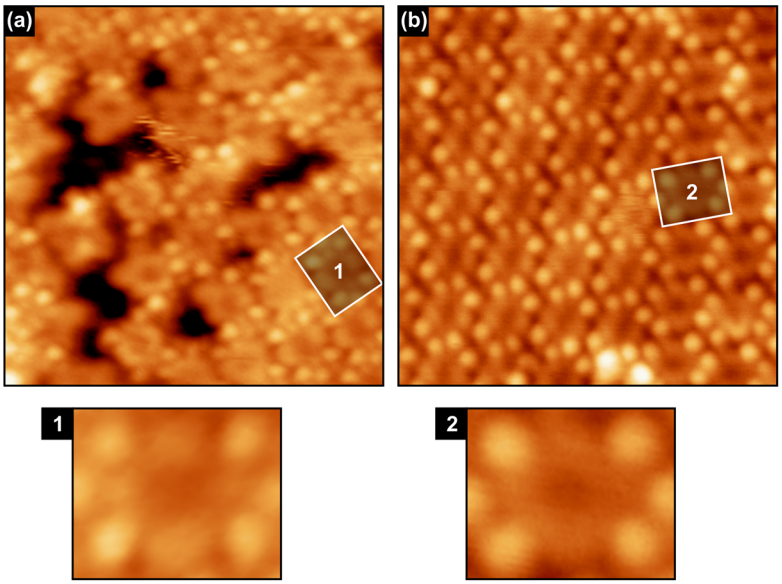

Fig. S5. (a) STM image of a Pb(TPP) monolayer after heating to 550 K and (b) of a H_2(TPP) monolayer after deposition at 300 K. The appearance of the demetalation product in (a) is compared to (b) H_2(TPP) by means of an enlarged image section in (1) and (2). Tunneling parameters and image sizes: (a) $U = -1.40$ V, $I = -0.14$ nA, 10×10 nm^2; (b) $U = -1.74$ V, $I = -0.16$ nA, 10×10 nm^2.

S7 Additional XPS spectra of the on-surface metalation of H2(TPP) with Pb and the on-surface reaction after thermal treatment

On-surface metalation. A H_2(TPP) monolayer was prepared on Au(111) by multilayer desorption at 520 K. The on-surface metalation was carried out by vapor deposition of Pb onto the initial H_2(TPP) monolayer. Pb pellets were heated to 840 K to achieve a Pb flux of 0.11 nm/min during deposition. The used amount of Pb is equivalent to a 0.03 nm metal film and corresponds to a coverage of 0.07 ML, which is approximately 1.7 times the amount of H_2(TPP) molecules in the initial monolayer. Fig. S3 show the corresponding N 1s and C 1s XPS signals before and after the deposition of Pb as well as the Pb $4f_{7/2}$ XPS signal. Although the metal was used in excess, an incomplete conversion H_2(TPP) → Pb(TPP) was obtained based on the N 1s signal. In line with this, the Pb signal shows the presence of a metallic Pb(0) signal in addition to the Pb(II) signal.

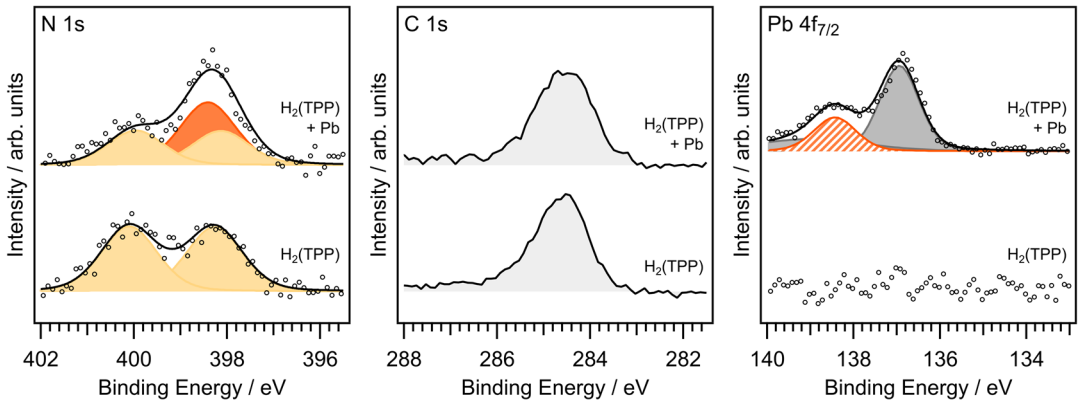

Fig. S6. XPS spectra of the initial H_2(TPP) monolayer on Au(111) (bottom spectra) and after deposition of Pb atoms (upper spectra). The N 1s signal intensity ratio of H_2(TPP) (beige) and Pb(TPP) (orange) indicates an incomplete reaction of about 50% conversion of the initial H_2(TPP). The deposition of Pb only leads to insignificant changes in the C 1s signature. In addition to the Pb(TPP) product peak (orange, dashed), the Pb $4f_{7/2}$ region contains a clearly visible Pb(0) peak at lower binding energies (gray).

On-surface reaction. Fig. S4 shows the XPS spectra of the in-situ metalated H_2(TPP) + Pb monolayer film after successive heating up to 550 K. As the temperature exceeds 470 K, the Pb $4f_{7/2}$ signal of the Pb(II) species is converted into additional Pb(0) signal intensity, indicating the reduction of the central Pb atom. The thermally induced reaction of the directly deposited monolayer suggests that this transformation results from porphyrin demetalation, in which the Pb center is released from the macrocycle. In addition, based on the Pb $4f_{7/2}$ signal, a conversion of the Pb↑ adsorbate structure into Pb↓ can be excluded, as the corresponding peak at 137.5 eV remains absent even at high temperatures.

While the C 1s signal shows no temperature-dependency, a clear change in the N 1s region is apparent. In particular, a shift in the ratio between the N 1s signal of unmetalated H_2(TPP) and the metalated species is evident. However, although the Pb $4f_{7/2}$ region suggests a complete demetalation and reduction of the Pb(II) centers, the N 1s spectrum clearly indicates that a substantial fraction of the porphyrins lack inner NH protons, i.e., the intensity of the unmetalated H_2(TPP) signal is not increased after heating to 470 K.

This behavior cannot be further clarified on the basis of the available experimental data. A possible, though speculative, explanation might be the excess of Pb atoms that catalyze the recombination of atomic H into H_2 and, thus, prevent the formation of unmetalated H_2(TPP).

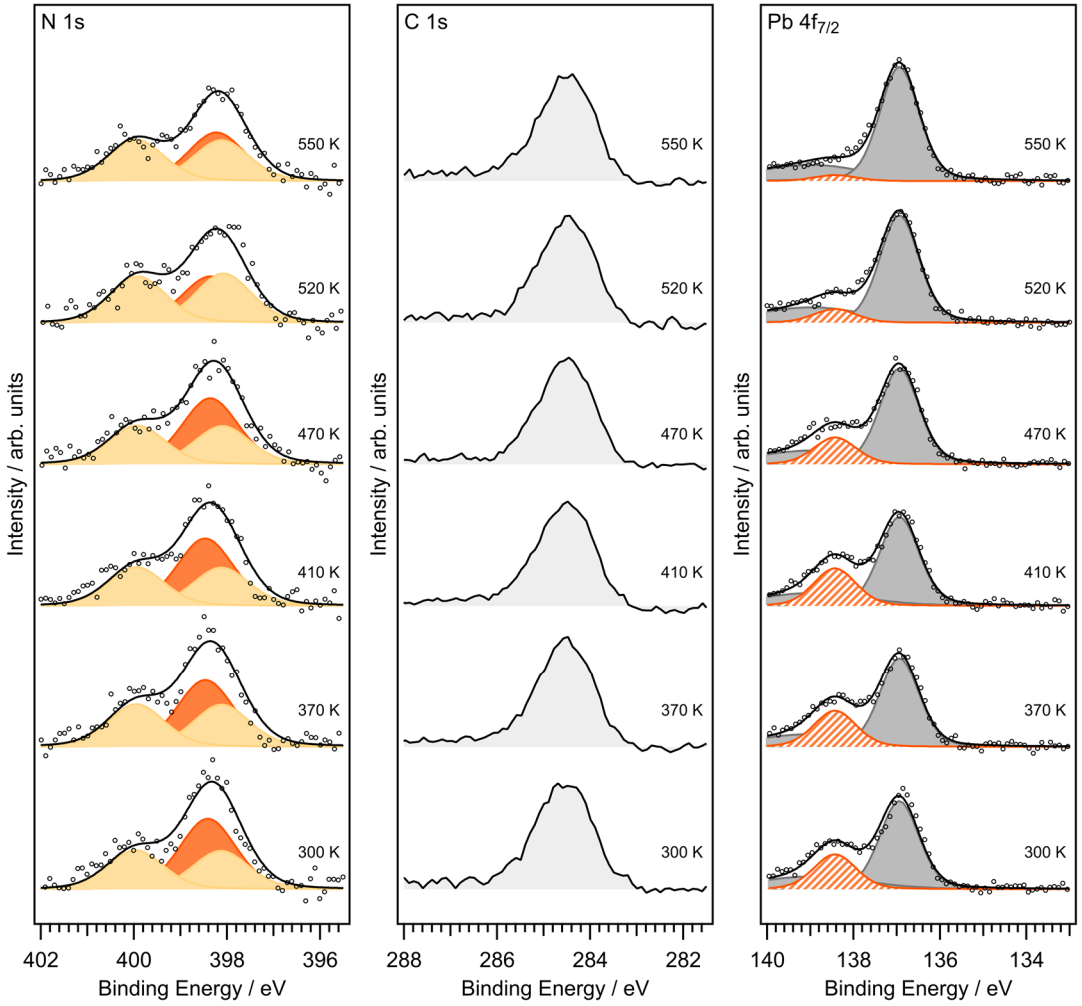

Fig. S7. Temperature-dependent N 1s, C 1s and Pb $4f_{7/2}$ spectra of the in-situ metalated H_2(TPP) monolayer with Pb after heating to the indicated temperatures. The N 1s region is described by the non-metalated H_2(TPP) species (beige) and the metalation product Pb(TPP) (orange). The Pb $4f_{7/2}$ region is constituted by the Pb(II) central atom of Pb(TPP) (orange, dashed) and the Pb(0) signal (gray).

References

1. M. J. Frisch, G. W. Trucks, H. B. Schlegel, G. E. Scuseria, M. A. Robb, J. R. Cheeseman, G. Scalmani, V. Barone, G. A. Petersson, H. Nakatsuji, X. Li, M. Caricato, A. V. Marenich, J. Bloino, B. G. Janesko, R. Gomperts, B. Mennucci, H. P. Hratchian, J. V. Ortiz, A. F. Izmaylov, J. L. Sonnenberg, D. Williams-Young, F. Ding, F. Lipparini, F. Egidi, J. Goings, B. Peng, A. Petrone, T. Henderson, D. Ranasinghe, V. G. Zakrzewski, J. Gao, N. Rega, G. Zheng, W. Liang, M. Hada, M. Ehara, K. Toyota, R. Fukuda, J. Hasegawa, M. Ishida, T. Nakajima, Y. Honda, O. Kitao, H. Nakai, T. Vreven, K. Throssell, J. J. A. Montgomery, J. E. Peralta, F. Ogliaro, M. J. Bearpark, J. J. Heyd, E. N. Brothers, K. N. Kudin, V. N. Staroverov, T. A. Keith, R. Kobayashi, J. Normand, K. Raghavachari, A. P. Rendell, J. C. Burant, S. S. Iyengar, J. Tomasi, M. Cossi, J. M. Millam, M. Klene, C. Adamo, R. Cammi, J. W. Ochterski, R. L. Martin, K. Morokuma, O. Farkas, J. B. Foresman and D. J. Fox, *Gaussian 16, Revision A.03, Gaussian, Inc., Wallingford CT*, 2016.
2. J. P. Perdew, K. Burke and M. Ernzerhof, *Phys. Rev. Lett.*, 1996, **77**, 3865-3868.
3. K. Eichkorn, F. Weigend, O. Treutler and R. Ahlrichs, *Theor. Chem. Acc.*, 1997, **97**, 119-124.
4. F. Weigend, M. Häser, H. Patzelt and R. Ahlrichs, *Chem. Phys. Lett.*, 1998, **294**, 143-152.
5. F. Weigend and R. Ahlrichs, *Phys. Chem. Chem. Phys.*, 2005, **7**, 3297-3305.
6. B. Metz, H. Stoll and M. Dolg, *J. Chem. Phys.*, 2000, **113**, 2563-2569.
7. C. Stadler, S. Hansen, I. Kröger, C. Kumpf and E. Umbach, *Nat. Phys.*, 2009, **5**, 153-158.
8. J. D. Baran and J. A. Larsson, *J. Phys. Chem. C*, 2012, **116**, 9487-9497.